Usage Report for Fiscal Year 2018

Project Title:

Prediction of Crystal Structure and Properties

Name: Yanming Ma (1), ○ Toshiaki Iitaka (1)
Laboratory at RIKEN:
(1) Computational Engineering Applications Unit, RIKEN

1. Background and purpose of the project, relationship of the project with other projects

Ternary phosphorus nitrides have received increasing interest owing to the possibilities for various applications, e.g., ionic conductors, hard materials and luminescent materials. As a characteristic structural unit, PN_4 tetrahedron is commonly found in these compounds, whose interconnection results in different crystal structure types, for example, isolated PN_4^{7-} anions in Li_7PN_4, $P_3N_9^{12-}$ rings in $Li_{12}P_3N_9$, $P_4N_{10}^{10-}$ cage in $Li_{10}P_4N_{10}$ and infinite PN_3^{4-} chains in Ca_2PN_3. The anionic three-dimensional (3D) network of vertex-sharing PN_4 tetrahedra has also been found in various ternary phosphorus nitrides, for example, APN_2 (with A being univalent cations Li, Na and Cu) and MP_2N_4 (with M being Ca, Sr and Ba). These 3D tetrahedral networks are of special interest because they might show structural analogies with SiO_2 and exhibit rich structural diversity at high pressure.

Solid-state reaction is a common method to synthesize ternary nitrides. The APN_2 crystal (with A=Li, Na and Cu) can be prepared by reactions of binary nitrides P_3N_5 and A_3N at different temperatures and pressures. Specifically, $LiPN_2$ can be obtained at 800 ℃, $NaPN_2$ at 1000 ℃ and 3 GPa, and $CuPN_2$ at 1000 ℃ and 5 GPa. The structural features, lattice dynamics, elastic properties and chemical bonds of them in the chalcopyrite-like structure have been thoroughly studied. For example, Basalaev *et. al.* revealed that $LiPN_2$ and $NaPN_2$ crystals take an intermediate position between the ideal configurations of β-cristobalite and chalcopyrite structure. Kosobutsky reported that the dynamical and elastic behavior of $LiPN_2$ and $NaPN_2$ is determined by the strong covalent P-N bond and the substantially weaker A-N interaction. Pucher *et. al.* showed that $LiPN_2$, $NaPN_2$ and $CuPN_2$ are indirect semiconductors with potential ceramic applications.

Pressure is a versatile thermodynamic variable to synthesize new structure, as well as to investigate the nature of chemical bond and atomic interactions. According to the pressure-coordination rule, high coordination numbers are likely to occur in high-pressure polymorphs. A good example is observed in SiO_2, which transforms from four-coordinated coesite to six-coordinated stishovite at high pressures. The similar coordination number changes of Si is also found in ternary metal silicates, e.g. the SiO_4 tetrahedron is replaced by the SiO_6 octahedron when ringwoodite dissociates into perovskite and ferripericlase at extreme pressures. Since the element combination P/N is isoelectronic with Si/O, the formation of high-coordinated phosphorus from PN_4 tetrahedra can thus be expected in highly compressed phosphorus nitrides. Indeed, pentacoordinate P has been experimentally realized in high-pressure polymorphs: γ-P_3N_5 and γ-HP_4N_7, and six-fold coordination environment for P have also been reported for hypothetic δ-P_3N_5 and spinel-type BeP_2N_4. These studies have generated great interest in the coordination chemistry of phosphorus and other metal elements in ternary phosphorus nitrides at high pressure.

2. Specific usage status of the system and calculation method

During the fiscal year 2018, we have used about 95% of the total allocated CPU hours and, the rest 5% will be used up at the end of this financial year. We searched for $CuPN_2$ structures through CALYPSO methodology as implemented in CALYPSO code.

Structure predictions with system sizes that ranging from 2 to 4 formula units per simulation cell were performed at pressures of 50, 100 and 150 GPa. The total energy calculations and local structural relaxations were carried out using the density functional theory as implemented in the VASP code. To deal with the effects of changing temperature on the Helmholtz free energy, we incorporated the effects of thermal vibrations (phonons) using PHONOPY code.

3. Result

The enthalpies of the most energetically competitive structures of $CuPN_2$ for the pressure range 0-160 GPa are presented in Fig. 1. At ambient pressure, the experimentally observed tI16 phase (space group $I\bar{4}2d$) has lower enthalpies than all other candidates, indicating that it is the thermodynamic ground state. Interestingly, two nearly energetically degenerate structures, hR4 and oC16, take over the stability at around 34 GPa. The hR4 structure is slightly more stable than the oC16 structure and the energy difference is about 1 meV at the pressure studied. The hR4 and oC16 structures exhibit a rather large pressure range of stability, and they transform to a hR4' structure at ~120 GPa. As a typical feature of a first-order phase transition, the volumes collapse by ~6.7 % and ~5.4 % in the tI16 → hR4/oC16 and hR4/oC16 → hR4' transitions, respectively. The pressure-induced decomposition of $CuPN_2$ to P_3N_5 and Cu_3N was further considered and negative formation enthalpies were found in the whole pressure range studied, which indicated the energetic stability of $CuPN_2$. The experimental α-P_3N_5 and γ-P_3N_5 and a hypothetic δ-P_3N_5 were chosen as the reference structures for P_3N_5, whereas the experimental anti-ReO_3 structure was chosen for Cu_3N.

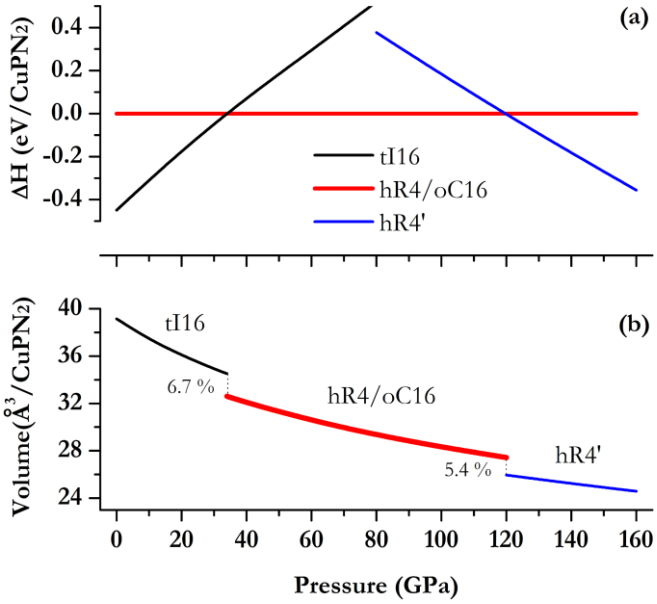

Figure 1

The experimental tI16 phase (space group: $I\bar{4}2d$; Z=4) is featured by a cristobalite-type P/N network, as shown in Fig. 2 (a). Each PN_4 tetrahedron is linked by means of shared corners with four neighboring PN_4 tetrahedra. At ambient pressure, structural parameters of tI16 in the tetragonal unit cell are: a = 4.492 and c = 7.760 Å, with Cu 4*a* (0, 0, 0), P 4*b* (0, 0, 0.5) and N 8*d* (0.666, 0.25, 0.125). Our theoretical results basically agree with the experimental values of a=4.503 Å and c=7.616 Å with the volume and c/a being overestimated by ~1.4% and ~2.1%, respectively. The PN_4 tetrahedron deviates slightly from the regular tetrahedron with N-P-N angles splitting into 108.48° and 109.97° and P-N distance of 1.660 Å. The CuN_4 tetrahedron is heavily distorted with N-Cu-N angles splitting into 102.19° and 125.30° with Cu-N distance of 2.111 Å. As a result, the CuN_4 tetrahedron looks flatter than the PN_4 tetrahedron along c axis. These angles for the PN_4 and CuN_4 tetrahedron do not depend very sensitive on pressure, e.g. the changes are less than 0.2 % and 1.2 % with pressure increasing to 34 GPa, however, the P-N and Cu-N distance decreases significantly by 2.9% and 5.7%, respectively, in the same pressure range.

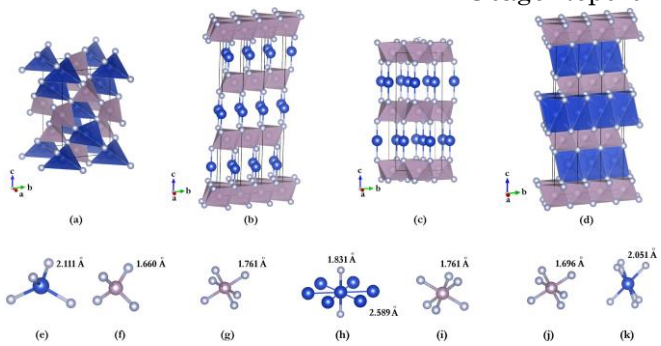

Figure 2

As shown in Fig. 2(b, c), both hR4 and oC16 structures consist of alternate layers of Cu atom and PN_2 sandwich stacked along the *c*-axis. Within each PN_2 slab, half of the octahedral voids are filled by P atoms which lead to the formation of an edge-sharing PN_6 octahedra network. The coordination number of N remains four, same as that of tI16, however, the coordination number of Cu changes from four to two. It seems that the PN_6 octahedron forms at the expense of the coordination number decrease of Cu atom. At 40 GPa, structural parameters of hR4 (space group: $R\bar{3}m$; Z=1) in the hexagonal cell is: a = 2.589 and c = 16.577 Å, with Cu 3*b* (0, 0, 0.5), P 3*a* (0, 0, 0) and N 6*c* (0, 0, 0.6105), whereas oC16 (space group: *Cmcm*; Z=4) in the orthorhombic unit cell are a = 2.589, b = 4.484 and c = 11.052 Å with Cu 4*c* (0, 0.3335, 0.25), P 4*a* (0, 0, 0) and N 8*f* (0, 0.1667, 0.0843). Interestingly, by shifting the Cu atom a little bit of ~0.0008 Å, oC16 could be described by the hexagonal $P6_3/mmc$ symmetry (a supergroup of *Cmcm*; Z=2) with structural parameters being a = 2.745 and c = 11.052 Å with Cu 2*c* (0.3333, 0.6667, 0.25), P 2*a* (0, 0, 0) and N 4*f* (0.3333, 0.6667, 0.9177). A transformation matrix which relates the coordinate system of oC16 to that of the $P6_3/mmc$ symmetry is (-*a*-*b*, *a*-*b*, *c*; 0, 0, 0). The oC16 and the hR4 exhibit many structural similarities, e.g., the edge-sharing PN_6 octahedra network, the coordination environment of Cu atom, the P-N distances (~1.761 Å) and the Cu-N distances (~1.831 Å), which explains why they have nearly degenerate enthalpies. It is clear that the different packing manner of PN_2 slabs of the two structures (see Fig.2) does not lead to large energy divergence. The P-N and Cu-N distance do not depend very sensitive on pressure, e.g. they decrease by 4.5 % and 5.0 %, respectively, with pressure increasing from 40 to 120 GPa.

An important structure feature of hR4' is that all atoms (Cu, P and N) are six-fold coordinated, which significantly differs from that of the low-pressure tI16 structure with all atoms being four-fold coordinated, or the hR4/oC16 structure with Cu, P and N atoms being two-, six- and four-fold coordinated, respectively. The high coordination numbers observed in the high-pressure polymorphs is in good agreement with the pressure-coordination rule. As shown in Fig. 2(d) and (b), hR4' and hR4 have similar CuP sublattice, and the major difference lies in that N atoms occupy the octahedral voids in the former, but the tetrahedral voids in the latter. The hR4' structure can be obtained from the hR4 structure by flipping over the PN_2 framework or equivalently shifting the N atom within the *ab* plane. At 140 GPa, structural parameters of hR4' (space group $R\bar{3}m$; Z=1) in the hexagonal cell are: a = 2.460 and c = 14.439 Å, with Cu 3*b* (0, 0, 0.5), P 3*a* (0, 0, 0) and N 6*c* (0, 0, 0.2691). The PN_6 octahedron deviates slightly from the regular octahedron with dihedral angles splitting into 110.96° and 107.94° and P-N distance of 1.696 Å. The CuN_6 octahedron is heavily distorted with dihedral angles splitting into 114.73° and 103.50° and Cu-N distance of 2.051 Å.

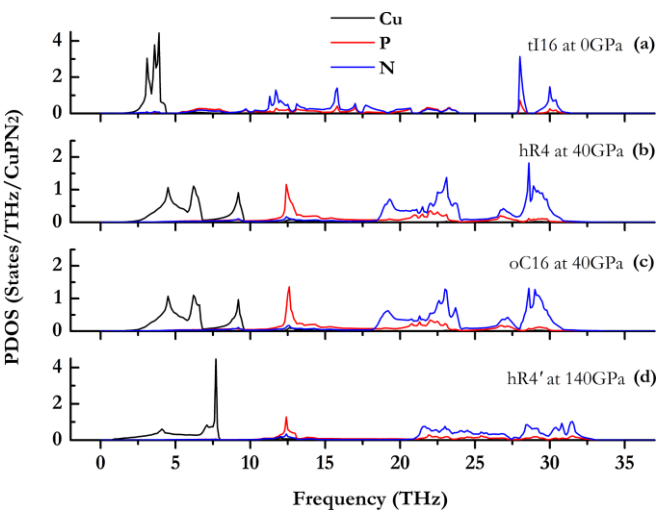

Figure 3

The phonon density of states (PDOS) projected on Cu, P and N atoms are shown in Figs. 3 for tI16, hR4/oC16 and hR4' at 0, 40 and 140 GPa, respectively. For all of them, the low- and high-frequency vibrational modes are dominated respectively by the heavy Cu element and light P/N element. For tI16, peaks of Cu atoms locate themselves at a relatively narrow region of 2.5-4.5 THz, whereas for P/N atoms the region is much wider and frequencies can reach as high as ~31 THz. The two peaks around 30 THz are attributed to the asymmetric stretching T2 mode of the PN_4 tetrahedron. For hR4/oC16, peaks of Cu atom clearly shift to higher frequencies with respect to tI16 because of the significant shortening of the Cu-N distance (by ~13 %). The third peak (at ~9 THz), showing the highest frequencies of Cu atoms, is attributed to the asymmetric stretching modes of the linear N-Cu-N bond. The last peak of hR4/oC16 is located at around 30 THz with no marked increase of the frequency in comparison with tI16. This is understandable considering that the P-N bond of the former is indeed ~6 % longer than that of the latter though the volume is reduced by ~18 %. The PDOS of hR4' is not quite different from hR4/oC16, except for the frequencies of the last peak dominated by Cu atom that is lowered by ~3 THz. We attribute this to the significant increasing of the Cu-N distance (~ 12 %). Moreover, we note that the peaks dominated by P atom for hR4' and hR4/oC16 are located in the same frequency region (~12.5 THz) though they have a large pressure difference of 100 GPa, which is a result of the strong configuration stability of the PN_6 octahedron.

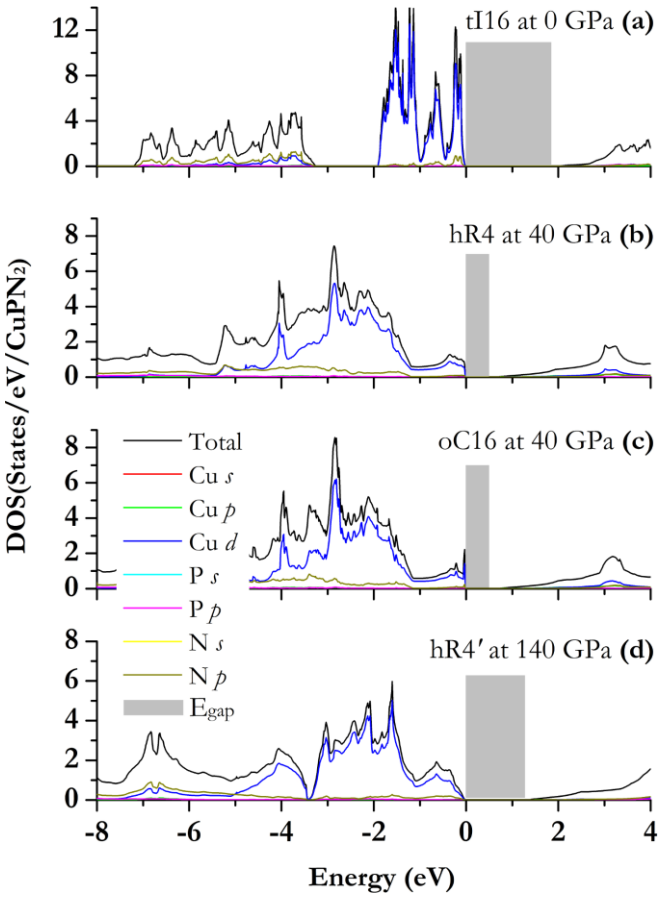

Figure 4

The appearance of energy gap (E_{gap}) in the electronic density of states (DOS) (Fig. 4) indicates that all four structures are semiconductors. For tI16 at 0 GPa, the calculated E_{gap} (1.84 eV) is ~9 % larger than that from LAPW method. We attribute this to the difference in the methods, and the slight overestimation of our volume and *c/a* with respect to the experiments. With pressure increasing to 34 GPa, the E_{gap} of tI16 decreases slightly to 1.82 eV. Further compression induces an unexpected large decrease of E_{gap} by 73 % to ~0.49 eV in the tI16 → hR4/oC16 transition, and moreover, an abnormal increase of E_{gap} by ~149 % from 0.46 to ~1.22 eV in the hR4/oC16 → hR4' transition at ~120 GPa. Generally speaking, E_{gap} of materials decreases with pressure increasing, and a sizable reduction of E_{gap} should come along with a significant collapse of volume in the first order structural phase transition of a nonmetal. To the best of our knowledge, this is the first report on the pressure-induced anomalous increase of E_{gap} in ternary phosphorus nitrides. To

understand the underlying mechanism, we have further studied the band structures and chemical bonds of those structures. Since hR4 and oC16 show similar electronic properties, only the former will be discussed here.

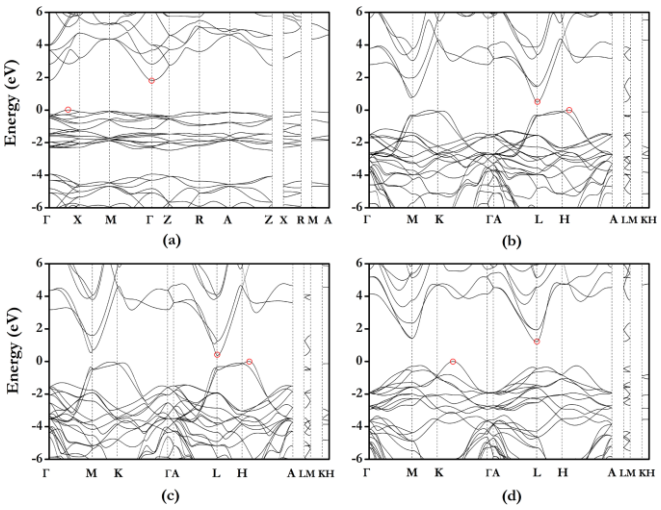

Figure 5

The band structures of tI16 at 34 GPa, hR4 at 34 and 120 GPa and hR4' at 120 GPa are shown in Fig. 5, which reveals that all of those structures have indirect energy gap. Top of the valance band (TVB) and bottom of the conduction band (BCB) are marked by red circles. The energy gap of tI16 is determined by TVB along Γ-X direction and BCB at Γ point. The hR4 and hR4' show BCB both at L point, however, possess TVB along H-A and K-Γ direction, respectively. The electron wave functions associated with the TVB and BCB illustrate clear Cu 3*d*, N 2*p* and P 3*p* orbital characters, for example, which can mainly be projected on N p_z and Cu d_{z2} orbital for TVB and Cu p_x and p_y orbital for BCB in hR4. It is therefore important to study the evolution of the Cu-N and P-N distance under pressure. As shown in Fig. 6, both of them decrease monotonically with pressure increasing within a single structure. The P-N distance increases by ~10 % and 2 % during the two phase transitions, whose trend does not agree with that of the energy gap. However, a decrease of ~7 % and an increase of ~19 % were found in the tI16 → hR4 and hR4 → hR4' transitions, respectively, which are clearly correlated to the changes of the energy gaps, indicating that the Cu-N distance plays a crucial role in determining the energy gap.

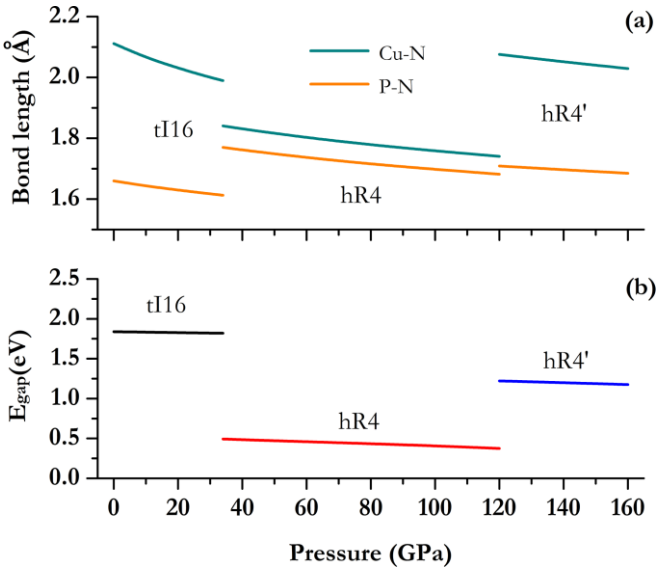

Figure 6

The Crystal Orbital Hamilton Population (COHP) analysis makes it possible to precisely study the nature of the chemical bonding by partitioning the band-structure energy into orbital-pair interactions. For tI16, hR4 and hR4' at 0, 40 and 140 GPa, the COHP of P-N and Cu-N bonds were calculated and shown in Fig. 7. A positive sign of COHP around the Fermi level indicates that the energy gap is determined by the antibonding interactions. The integrated COHP (ICOHP) can provide an estimate of the net strength of the bonding between a pair of atoms. The ICOHP of P-N pairs is negative and decreases from tI16 (-8.4 eV) to hR4 (-6.2 eV) and hR4' (-6.7 eV), which reveals that the P-N bond of the 4-fold P is slightly stronger than that of the 6-fold P atom. Unexpectedly, for Cu-N bond, a value of -2.5 eV has been found in hR4, which is about 2 and 2.7 times that of tI16 (-1.26 eV) and hR4' (-0.92 eV), respectively, indicating that the 2-fold Cu atom has Cu-N bonds much stronger than the 4- and 6-fold Cu atom in these structures. This result was independently double-checked by the quantum theory of atoms in molecule. With the calculated critical points fulfilling Morse's topological relationship, bond critical points (BCP) were found in the nearest Cu-N pairs. Remarkably, a negative

Laplacian ($\nabla^2\rho(r) < 0$) was found at it in hR4 structure to indicate a shared-shell covalent Cu-N interaction. Owing to the covalent nature of both Cu–N and P–N bonds, tI16-$CuPN_2$ was classified as a double nitride. Accordingly, the high-pressure polymorphs can also be regarded as double nitrides and not the Cu nitridophosphate.

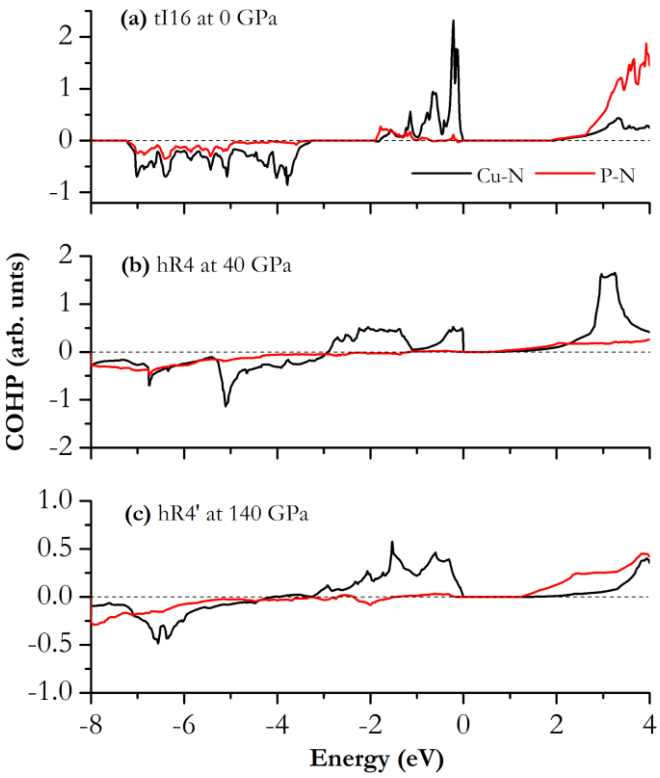

Figure 7

4. Conclusion

The present study explored the structural and electronic properties of double nitrides $CuPN_2$ over a wide pressure range of 0–160 GPa using an efficient structure search method in combination with first-principles calculations. Two pressure-induced structural transformations were predicted, as tI16 → hR4/oC16 → hR4' at 34 and 120 GPa, respectively. An important structure feature of the nearly energetically degenerate hR4 and oC16 structures is that Cu atom adopts a two-fold coordinated environment, which is lower than both of the low-pressure tI16 structure (with four-fold Cu atom) and the high-pressure hR4' structure (with six-fold Cu atom). Electronic structure calculations reveal that all of those structures are semiconductors with indirect energy gap. The energy gap exhibits remarkably large decrease of ~73 % and an abnormal increase of ~149 % in the two structural transitions, respectively. This trend is clearly correlated to the unusual changes of the Cu-N distance in the structural transitions, i.e. decreasing in the first while increasing in the second, which suggest that the Cu-N environment plays a crucial role in determining the energy gap. The current work indicates that the coordination chemistry of metal elements in ternary phosphorus nitrides may be much more complex than what it looks at the first sight.

5. Schedule and prospect for the future

I have been a HOKUSAI general user and wish to continue using the system. During the last fiscal year 2018, I have published one paper on the high-pressure behaviors of $CuPN_2$, and another paper on the high-pressure properties of FeXn (X=Cl, Br and I, n =1/4, 1/3,1/2, 1, 2, 3, 4) system that had been reported last year. For the next fiscal year 2017, we plan to continue using HOKUSAI supercomputer to study the high-pressure polymorphism of nitratine through CALYPSO code, and build the high-pressure phase diagram. We expect high standard publications can be eventually achieved.

Usage Report for Fiscal Year 2018

Fiscal Year 2018 List of Publications Resulting from the Use of the supercomputer

1. DanXu, Bingtan Li, Toshiaki Iitaka, Qiliang Cui, Hongbo Wang, and Hui Wang, **Exotic high-pressure behavior of double nitride $CuPN_2$**, *Computational Materials Science*, 152, 217-222 (2018).
2. Xiangpo Du, Ziwei Wang, Hongbo Wang, Toshiaki Iitaka, Yuanming Pan, Hui Wang, and John S Tse, **Structures and Stability of Iron Halides at the Earth's mantle and core pressures: Implications for the missing halogen paradox**, *ACS Earth Space Chem.* 2, 711 (2018).